Volume 1 | Number 1 | Jan 2013 | Pages 1–100

Journal of
Materials Chemistry B

Materials for biology and medicine
www.rsc.org/materialsB

ROYAL SOCIETY
OF CHEMISTRY

ROYAL SOCIETY
OF CHEMISTRY

www.rsc.org/materialsB

Journal of Materials Chemistry B

ARTICLE

Highly flexible heparin-modified chitosan/graphene oxide hybrid hydrogel as a super bilirubin adsorbent with excellent hemocompatibility

Houliang Wei,[a] Lulu Han,[a] Yongchao Tang,[b] Jun Ren,[a] Zongbin Zhao[b] and Lingyun Jia*[a]

As a pathogenic toxin, bilirubin is generally removed from blood by hemoperfusion for the remission of liver disease and striving time for liver transplantation. However, the development of bilirubin adsorbents with excellent mechanical property, adsorption performance and hemocompatibility is still a big challenge. In this work, a heparin-modified chitosan/graphene oxide hybrid hydrogel (hep-CS/GH) has been developed for bilirubin adsorption by a lyophilization-neutralization-modification strategy. The as-prepared hybrid hydrogel displayed a unique foam-like porous structure and excellent mechanical flexibility. It was revealed that the incorporation of GO into the chitosan matrix enhanced both the compressive strength and Young's modulus of the hybrid hydrogel, as well as its adsorption capacity for bilirubin. The maximum adsorption capacity of hep-CS/GH for bilirubin was 92.59 mg/g, according to Langmuir isotherm model. We demonstrated that hep-CS/GH performed high adsorption selectivity for bilirubin against albumin, and could effectively adsorb bilirubin from bilirubin-enriched serum. After the hydrogel was modified with heparin, protein adsorption, platelet adhesion and hemolysis were reduced, and the plasma clotting time was prolonged from 4.1 to 23.6 min, indicating a better hemocompatibility of hep-CS/GH. Therefore, this study may pave a significant way for improving the performance of the adsorbent for blood toxins removal.

Introduction

Bilirubin, one of the metabolites of hemoglobin, is a hydrophobic pathogenic toxin that binds to albumin (Fig. S1). It is transported in the bloodstream to the liver for conjugation with glucuronic acid and excreted into the bile.[1] However, bilirubin would be accumulated in blood once patients suffer from a liver disease, such as acute liver failure, resulting hyperbilirubinnemia. As a result, the extra free bilirubin can deposit into various tissues including brain tissues, which leads to hepatic coma or even death,[2] because of the high toxicity of bilirubin to many cell types.[3] Therefore, removal of excess bilirubin from blood is important for the remission of liver disease and striving time for liver transplantation. Hemoperfusion, an extracorporeal blood-circulation device containing adsorbents, is one of the most effective techniques for bilirubin removal.[4] Until now, many kinds of adsorbents, such as activated carbon, resins, carbon nanotubes and mesoporous silica, have been exploited.[3, 5-7] However, these adsorbents have problems of unsatisfied adsorption performance, and/or low hemocompatibility. All of these adsorbents have no anticoagulant activity, which means that a high dose of heparin needs to be administrated by intravenous injection to prevent blood coagulation, and this may put the patients at high risk of bleeding or other severe side effects.[8]

Therefore, bilirubin adsorbents with excellent adsorption performance and hemocompatibility, especially anticoagulant activity, are in strong demand.

Graphene oxide (GO), a kind of the graphene derivative, has received tremendous attention as adsorbents for many organic compounds due to its huge surface areas (e.g., theoretical value for graphene is 2630 m^2/g).[9] Besides, it possesses rich oxygen-containing groups and delocalized π-electron region for the formation of hydrogen bond, electrostatic attraction and/or π-π interaction with organic compounds.[9] Recently, various GO-based adsorbents have been investigated for highly effective removal of pollutants from contaminated water.[10-12] Hence, it is reasonable to take advantage of the strong adsorption ability of GO to develop novel GO-based adsorbents in hemoperfusion for bilirubin removal. However, the low blood compatibility of GO hampers its application in hemoperfusion. GO might induce blood coagulation and hemolysis once it contacts blood.[13] In addition, GO exhibits a dose-dependent toxicity,[14-15] and the leakage of GO into blood might be harmful to patients. Although GO could self-assemble into a three-dimensional architecture or hydrogel under reducing conditions,[16] the resulted hydrogel is brittle.

To overcome these obstacles, preparing the GO-based composite materials with biocompatible polymers may be a better choice. GO could self-assemble with polymers to form a

3D architectures[17-20]. Chitosan is a natural polyglucosamine, deriving from the deacetylation of chitin. It has been used to fabricate tissue engineering scaffolds and matrices for controlled release of drugs, because of its good biocompatibility, antimicrobial properties and low toxicity.[21] In earlier reports, several chitosan monoliths doped with GO have been prepared for wastewater treatment or drug delivery by various methods,[22-25] demonstrating that these composites also possess adsorption ability as GO. However, chitosan has been found to promote blood coagulation in vitro.[26] Heparin, a highly sulphated linear polysaccharide, has been widely used to functionalize the surfaces of blood-contacting materials due to its ability to inactivate blood coagulation path ways.[27] Therefore, modification of chitosan with heparin would be an effective solution to improve the anticoagulant activity of chitosan/GO composites.

In this work, a heparin-modified chitosan/GO hybrid hydrogel (hep-CS/GH) was prepared through a lyophilization-neutralization-modification method, and for the first time, used as a blood compatible adsorbent for bilirubin removal. We demonstrated that the hybrid hydrogel was highly flexible with high adsorption capacity and selectivity for bilirubin, as well as good hemocompatibility.

Experimental

Materials

Graphite powder (180 mesh) was purchased from Qingdao Black Dragon Graphite Co. Ltd.(China). Chitosan (CS, Mw ~ 100 kDa) was provided by Jinan Haidebei Marine Co. Ltd. (China). Heparin (sodium salt, 140 IU/mg) and bovine serum albumin (BSA) were obtained from Beijing Solarbio Science & Technology Co., Ltd. (China). 1-(3-Dimethylaminopropyl)-3-ethylcarbodiimide hydrochloride (EDC•HCl) and N-Hydroxysuccinimide (NHS) were bought from GL biochem. Ltd. (Shanghai, China) and Aladdin-reagent (Shanghai, China), respectively. Human fibrinogen was supplied by Shanghai Xinxing Medicine Co. Ltd. (China). Bilirubin was purchased from Maikun Chemical Company (Shanghai, China). Human serum was provided by Blood Bank of Dalian (China). Deionized water was obtained from a Milli-Q ultrapure water purification system (Millipore; Billerica, USA). All other chemicals were of analytical grade.

Preparation of heparin-modified chitosan/GO hybrid hydrogel

GO was prepared via a modified Hummers' method according to our previous report.[28] In a typical process for the preparation of the hydrogel, 300 mg of chitosan was dispersed into 10 mL of 3 mg/mL GO suspension, and then 0.2 mL of acetic acid was added. The mixture was vigorously stirred to make the chitosan dissolved, and then the bubbles in the mixture were removed by vacuum degassing. Thereafter, the mixture was poured into a mold and freeze-dried under vacuum. The obtained porous structures were immersed in 0.5 M NaOH solution to remove the excess acid, and then thoroughly washed with deionized water. The resulted hydrogel was denoted as chitosan/GO hydrogel (CS/GH). Similarly, the chitosan hydrogel (CSH) in the absence of GO and the CS/GH with different GO content were also prepared.

Coupling of heparin on CS/GH was performed using EDC and NHS. First, 30 mg of heparin, 9 mg of NHS, and 30 mg of EDC•HCl were dissolved in 20 mL of phosphate buffer solution (50 mM, pH 5.5) in sequence. After reaction for 1 h in a shaker, the pH of the solution was set to 7.4, and then the solution was incubated with 150 mg of CS/GH (dry weight) overnight under shake. Excess reagents and physically bound heparin were removed by extensive washing with 2 M NaCl solution and deionized water.

Toluidine blue staining was performed to illustrate the coupled heparin. The heparin-modified CSH was prepared and stained by toluidine blue. Toluidine blue solution of 50 mg/L was prepared by adding 10 mg of toluidine blue O (Amresco, 0672) and 1 g of NaCl into 200 mL of deionized water. For comparison, the heparin-adsorbed CSH was also prepared under the same procedure without adding EDC/NHS in heparin solution.

Characterizations

The porous structure of the hydrogels was firstly observed by an optical microscope (Olympus IX71). Then, the samples were freeze-dried and observed by a scanning electron microscope (SEM, QUANTA 450) at 20 kV after coating with gold. X-ray diffraction (XRD) patterns were recorded on a Rigaku D/Max 2400 diffractometer. Attenuated total reflectance fourier transform infrared (ATR-FTIR) spectra of the freeze-dried hydrogels were obtained with a Nicolet-20DXB spectrometer. Elemental analysis was conducted with Elemental Analyzer Vario EL III. The compressive test was performed via a method reported previously,[29] and the schematic equipment is shown in Fig. S2.

Adsorption Experiments

Bilirubin in aqueous solution was prepared by dissolving 10 mg of bilirubin in 1 mL of 0.1 M NaOH solution. The bilirubin solution was then diluted to a certain concentration by 10 mM phosphate buffer saline (PBS, containing 0.15 M NaCl) with a final pH of 7.4. The effect of GO content on the adsorption of bilirubin was performed by adding 25 mg of hydrogel (dry weight) into 8 mL of bilirubin solution with an initial concentration of 300 mg/L. In kinetic experiments, 100 mg of hydrogel was added into a brown bottle containing 30 mL of 300 mg/L bilirubin PBS solution under shaking at 30°C. The concentrations of bilirubin were measured at different time intervals from 0.5 to 4 h. Bilirubin adsorption isotherm was obtained by incubating 25 mg of hep-CS/GH with 8 mL bilirubin PBS solution with different initial concentration of bilirubin at 30°C for 3 h. The concentration of bilirubin was analyzed by UV-vis absorption spectroscopy at a wavelength of 438 nm.

Removal of bilirubin from albumin solution and serum

Solid bilirubin was dissolved in 0.1 M NaOH solution, and added into BSA solution or human serum. For removal of bilirubin from albumin solution, 50 mg of hydrogel was incubated with 8 mL of bilirubin-enriched BSA solution with the initial bilirubin concentration of 516 μmol/L. The initial BSA concentrations were 258 μmol/L and 516 μmol/L, which resulted that the molar ratios of bilirubin to BSA were 2:1, and 1:1, respectively. After 4 h of adsorption, the bilirubin concentrations and BSA concentrations were analyzed by UV-vis absorption spectroscopy at 460 nm and 280 nm,[4] respectively. The number ratio (t_N) of the bilirubin molecules to the albumin molecules adsorbed on the hydrogel was calculated using the following equation:

$$t_N = \frac{C_{b0} - C_b}{C_{a0} - C_a}$$

where C_{b0} and C_b (μmol/L) are the bilirubin concentrations before and after adsorption; C_{a0} and C_a (μmol/L) are the BSA concentrations before and after adsorption.

For removal of bilirubin from serum, 50 mg of hydrogel was incubated with 8 mL of bilirubin-enriched serum with the initial bilirubin concentration of 305.4 mg/L and 153. 4 mg/L and shaken at $37^{o}C$. These initial concentrations are in the range of bilirubin concentration of the patients suffering from hyperbilirubinemia. The concentrations of bilirubin, albumin and total protein in the serum before and after adsorption were quantified on a semiautomatic biochemistry analyzer (RT-9000, Rayto, China) with the corresponding reagent kits (BioSino Bio-technology and Science Inc, China).

Protein adsorption

Protein adsorption experiments were firstly performed with BSA or fibrinogen solutions under static condition. The hydrogel (20 mg, dry weight) was incubated into 2 mL of 1 mg/mL BSA or fibrinogen solution (in PBS, pH7.4) at $37^{o}C$ for 4 h. The concentration of protein solution after adsorption was determined using a spectrophotometer at 280 nm. The amount of adsorbed protein on the hydrogel was calculated from the difference between this value and the original protein concentration.

Then, protein adsorption from plasma was also carried out. Fresh blood, obtained from a healthy rabbit (Laboratory Animal Center of Dalian Medical University), was mixed with the anticoagulant (0.129 M citrate, ratio of anticoagulant to blood 1:9).[30] All animal experiments were conducted in accordance with the guidelines for the Care and Use of Laboratory Animals from National Institute of Health, and approved by the Ethics Committee of Dalian University of Technology.

The blood was centrifuged at $2500 \times g$ for 15 min, and the resultant supernatant, as the platelet-poor plasma (PPP), was diluted five times with PBS. The hydrogel (20 mg) was incubated with 2 mL of the diluted PPP at $37^{o}C$ for 4 h, and washed thoroughly with PBS. After that, the adsorbed protein was eluted by 10% SDS solutions overnight, and then analyzed by SDS-polyacrylamide gel electrophoresis (SDS-PAGE) using Tris•HCl 12% (w/v) polyacrylamide gels under reducing condition. The gray value of the band intensity, representing the amount of adsorbed protein, was analyzed with the software of Image J.

Platelets adhesion

After centrifugation of the anticoagulated blood at $200 \times g$ for 5 min, platelet-rich plasma (PRP) was generated from the centrifugation supernatant. Platelet adhesion on the hydrogel was performed by mixing each sample with PRP for 1 h at $37^{o}C$. After washed with PBS for three times, the platelet-adhered hydrogels were fixed with 2.5 wt% glutaraldehyde solution for 2 h, and then dehydrated by 50, 70, 80, 90 and 100% (v/v) ethanol solution in sequence. The hydrogels were finally dried at room temperature, and the adherent platelets were observed with SEM. The platelet adhesion was quantified by counting the platelets adhered on each sample from six randomly selected SEM images, and the statistical analyses were assessed using Student's t-test. Statistical significance was accepted at $p < 0.05$.

Plasma recalcification time (PRT)

The anticoagulant activity of the hydrogels was determined by the plasma recalcification time (PRT) assay. $CaCl_2$ solution (25 mM) was preheated at $37^{o}C$. The hydrogel was placed into a tube, followed by the addition of 0.2 mL of PPP, and warmed at $37^{o}C$ for 3 min. Then, 0.2 mL of 25 mM $CaCl_2$ solution was added, and the tube was shaken in a $37^{o}C$ water bath. The time at the first appearance of silky fibrin was recorded as the PRT.

Hemolysis test

Hemolysis rate was evaluated by incubation of the hydrogel in diluted blood containing 5% fresh anticoagulant blood and 95% normal saline at $37^{o}C$ for 1 h. The diluted blood with 95% normal saline and deionized water in the absence of hydrogel were used as negative and positive controls. After centrifugation at $1000 \times g$ for 5 min, the absorbance of the supernatant at 541 nm was recorded. Hemolysis rate was calculated according to the following equation: Hemolysis rate (%) = $(A1-A3)/(A2-A3)\times100\%$, in which A1, A2, and A3 are the absorbances of the sample, positive control, and negative control, respectively.

Results and discussion

Characterizations of the hydrogels

Chitosan is a cationic natural polymer with hydroxyl and amino groups, and GO is negatively charged with carboxyls, hydroxyls and epoxides. The mixture of them can form a complex via electrostatic attraction and hydrogen bond.[31] The process for the preparation of hep-CS/GH included three main steps, as illustrated in Fig. 1a. First, CS/GO mixture in acetic acid aqueous solution was freeze-dried to produce a foam-like porous scaffold. In this step, chitosan/GO complex as a continuous phase was segmented during the phase separation of ice crystals,[32] inducing the generation of a highly foam-like porous scaffold after simultaneous sublimation of the ice. Then, this scaffold was fixed by immersing it into a strong alkaline solution to neutralize the remaining acetic acid, forming CS/GH. The porous structure in CS/GH was still maintained under wet state (Fig. S3), because almost no chitosan can be dissolved in the neutral or alkaline solutions. It is known that heparin is a highly sulphated linear polysaccharide which has been widely used to functionalize biomaterials to improve their blood compatibility.[27] In order to avoid the chitosan-induced blood coagulation, CS/GH was further modified with heparin to produce hep-CS/GH. The carboxyl groups of heparin were activated by EDC/NHS, and coupled to the amino groups of chitosan by amide bond.
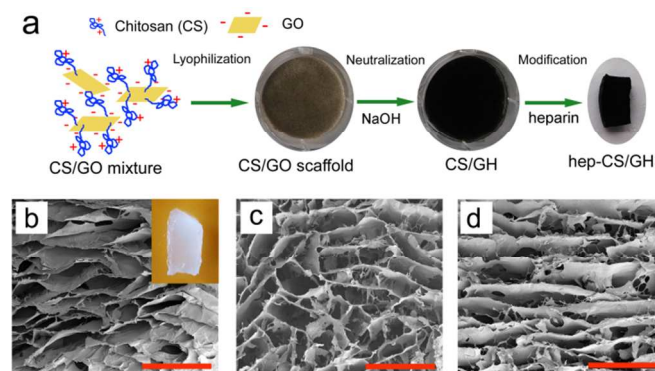
Fig. 1 (a) Schematic illustration of the process for the preparation of hep-CS/GH; SEM images of the hydrogels (scale bar 500 μm): (b) CSH (Inset was the digital image of CSH), (c) CS/GH, and (d) hep-CS/GH.

The structures of the generated hydrogels were investigated by SEM. Fig. 1b-d reveal that CSH, CS/GH and hep-CS/GH possess foam-like structures containing interconnected macropores in the range of tens to hundreds of microns. The CSH displayed the white color (inset of Fig. 1b), while the color of CS/GH was black (Fig. 1a), indicating that GO was

homogeneously dispersed in the chitosan matrix. The XRD patterns of the CSH, CS/GH and hep-CS/GH all exhibited a broad peak centered at 20.3° (Fig. S4), which represents the generally amorphous state of the CS.[23] The three XRD patterns were exactly the same, demonstrating that GO incorporation and heparin coupling had no influence on the crystalline properties of chitosan.

Fig. 2a shows the FTIR spectra of CSH, CS/GH and hep-CS/GH. No obvious changes were observed after GO incorporation. After coupling, the peak at 1261 cm^{-1} of CS/GH was shifted to an enhanced and widen peak at 1251 cm^{-1}, probably due to the overlapping of the peak at 1261 cm^{-1} of CS/GH and the peak at 1236 cm^{-1} (S=O) of heparin, suggesting the presence of heparin in hep-CS/GH.
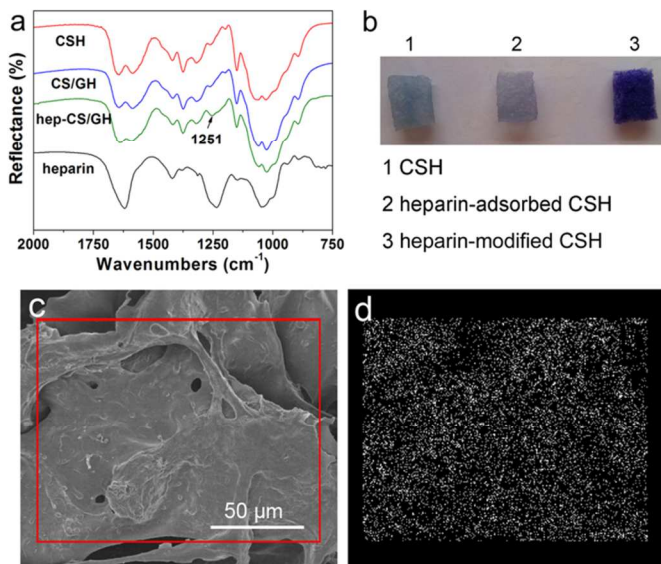
Fig. 2 (a) FTIR spectra of CSH, CS/GH and hep-CS/GH, (b) Digital image of toluidine blue staining, (c) SEM image and (d) sulfur mapping image of hep-CS/GH.

Moreover, toluidine blue staining was further performed to illustrate the successful heparin coupling based on the formation of a purple complex resulting from the interaction between toluidine blue and heparin.[33] The heparin-modified CSH in the absence of GO was used for staining to exclude the colored interference of the black hep-CS/GH. After staining, the CSH without heparin was light blue, while the heparin-modified CSH became deep purple (Fig. 2b). As a control, the CSH treated with heparin solution without EDC/NHS (heparin-adsorbed CSH) displayed light purple color, because only a small amount of heparin was physically adsorbed on chitosan. These results demonstrated that heparin was mainly covalently coupled to the chitosan in hep-CS/GH.

Elemental mapping images obtained from energy-dispersive X-ray (EDX) spectra were utilized to show the elemental distributions of sulfur in CS/GH (Fig. S5) and hep-CS/GH (Fig. 2c-d). The elemental mapping image of hep-CS/GH displayed the existence of sulfur which was distributed homogenously, thus indicating the uniform distribution of heparin on the wall surfaces of hep-CS/GH. Finally, elemental analysis was performed to quantify the amount of heparin in hep-CS/GH. The content of sulfur element was found to be 0.67 wt.%, so the coupling amount of heparin to chitosan is 5.87 wt.% in hep-CS/GH.

Mechanical flexibility

In contrast to the brittle nature of traditional hydrogels,[34] CSH, CS/GH and hep-CS/GH displayed extraordinary mechanical flexibility, which allowed for large deformations and shape recovery. Fig. 3a illustrates that the compressive strength of the CS/GH was much higher than that of the CSH. The Young's modulus of the hydrogel increased from 2.04 kPa to 12.6 kPa after GO incorporation (9.09 wt.% of GO). This reinforcement could be due to the cooperative contributions of inherently superior strength of GO and strong interactions between chitosan and GO sheets. Similar phenomenon is also observed in GO/DNA self-assembled hydrogel.[20] GO is a high surface area and high modulus filler with superior strength.[20, 35] Pervious research has shown that incorporation of GO could dramatically alter the stress dissipation, leading to improving the mechanical strength of the composites.[35-36] After the heparin was coupled, the hep-CS/GH exhibited the same flexibility as CS/GH. Fig. 3b shows that hep-CS/GH could be compressed and then recovered its original volume after releasing the external force. Besides, when the water in hep-CS/GH was squeezed out, the compressed hep-CS/GH could be folded into various forms, and then able to recover its original shape once uptaking the water again (Fig. 3c, Fig. S6). Fig. 3d shows that hep-CS/GH could bear a compressive strain as high as 80% and almost recover its original volume. Then, the hep-CS/GH was subjected to a cyclic compression test with 50% strain (Fig. 3e). The thickness reduction after 100 loading/unloading cycles was less than 10%. This extraordinary flexibility is mainly ascribed to the processes of lyophilization and neutralization, endowing the hydrogel with a foam-like porous structure under wet state (Fig. S3). With this structure, the as-prepared hydrogel exhibited excellent mechanical flexibility, even after surface modification such as heparin coupling. The excellent mechanical flexibility of hep-CS/GH is very beneficial for the safety concern in its practical applications.
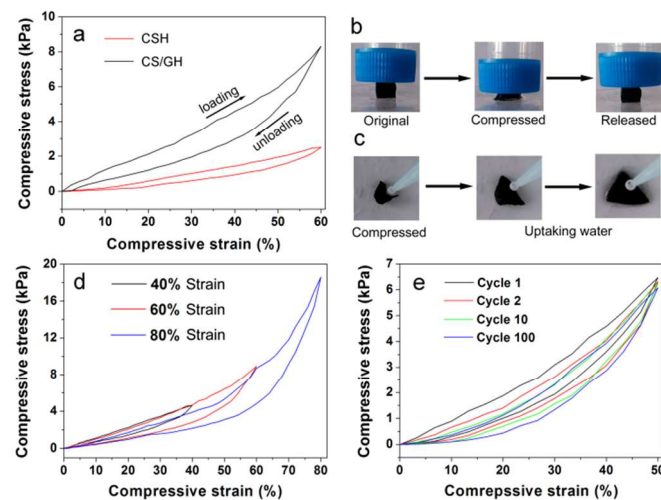
Fig. 3 (a) Stress-strain curves of CSH and CS/GH, (b) Digital images of a manual compression and releasing process of a hydrated hep-CS/GH, (c) Digital images of a shape recovery process after uptaking water of a compressed dehydrated hep-CS/GH. Stress-strain curves of hep-CS/GH: (d) at different maximum strains; (e) at a strain of 50% for different cycles.

Adsorption properties of hep-CS/GH for bilirubin

The effect of GO content on the adsorption of bilirubin was investigated (Fig. 4). Fig. 4 shows that the adsorption capacity of CS/GH for bilirubin in PBS was significantly improved with the increasing of GO content. For the CS/GH doped with 9.09 wt.% GO, its adsorption capacity was as high as 80.3 mg/g, about 4 times that of the CSH (20.4 mg/g). These results illustrate that GO played the crucial role in the adsorption of bilirubin. However, with the further increase of GO content, the CS/GO mixture was too sticky to form a homogeneous mixture during the preparation process. Therefore, CS/GH (9.09 wt.% of GO) was selected for our following study. The adsorption mechanism between GO and bilirubin may be owing to hydrogen bonding and π-π interaction between the C=C bonds of bilirubin (Fig. S1) and the GO planes.[10] Besides, it has been reported that chitosan could also adsorb bilirubin by its amino groups through electrostatic attraction.[37]
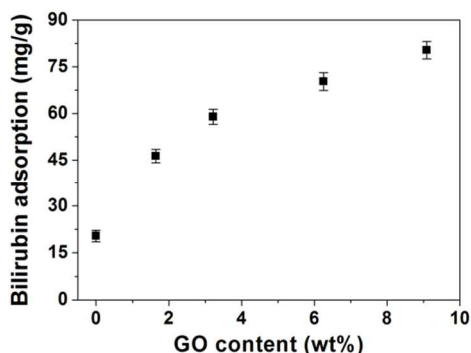
Fig. 4 Adsorption of bilirubin by CS/GH with different GO content (mean ± S.D, n = 3).

The kinetic adsorption of bilirubin by CS/GH and hep-CS/GH was studied. The adsorption capacity of hydrogels for bilirubin increased quickly in the first 0.5 h and then gradually reached maximum within 3 h (Fig. 5a). Besides, the adsorption capacity of the hep-CS/GH was slightly lower than that of the CS/GH, possibly due to the blockage of the amino groups of chitosan by heparin coupling and the electrostatic repulsion between heparin and bilirubin. Moreover, the hydrogels are very stable, and maintain their form and integrity in the process of adsorption.

Equilibrium adsorption isotherm of bilirubin onto hep-CS/G was shown in Fig. 5b. The adsorption capacity of hep-CS/GH improved with increasing equilibrium concentration of bilirubin and gradually reached saturation level. Two adsorption isotherm models, Langmuir and Freundlich isotherms, were used to fit the experimental data (see in Supporting information). The relative parameters calculated from Langmuir and Freundlich models were listed in Table S1. Based on the comparison of the correlation coefficient R^2 values, the Langmuir model fitted the adsorption data better than the Freundlich model. In other words, the adsorption of bilirubin by hep-CS/GH was in a monolayer adsorption manner. The maximum adsorption capacity obtained from Langmuir isotherm model was 92.6 mg/g, which outperformed many other reported bilirubin adsorbents, including activated carbon (70 mg/g),[38] Polyamidoamine Dendrons-modified Chitosan Microspheres (43 mg/g),[39] albumin-modified membrane (25 mg/g),[40] and arginine-modified composite membrane (52.6 mg/g).[41]

Bilirubin removal from albumin solution and serum

Bilirubin is a hydrophobic toxin and commonly binds with albumin in blood to form bilirubin-albumin conjugate.[1] Albumin is the natural carrier of bilirubin in the blood, and one albumin molecule can bind two bilirubin molecules.[41] For successful removal of bilirubin, an adsorbent should be able to competitively adsorb bilirubin with albumin. In this study, the adsorption of bilirubin on the hydrogels was investigated under two molar ratios of bilirubin to BSA in albumin solutions. As shown in Fig. 5c, when the molar ratio of bilirubin to BSA decreased from 2:1 to 1:1, which meant that the albumin concentration increased, the number ratio (t_N) of bilirubin molecules to albumin molecules adsorbed on the hydrogels decreased significantly. However, the t_N of bilirubin molecules to albumin molecules adsorbed on hep-CS/GH were still much larger than 2 under the two molar ratios. These results demonstrated that hep-CS/GH could compete with albumin for binding bilirubin and perform high adsorption selectivity for bilirubin against albumin. Similar phenomenon was also reported in other related researches.[42] It is generally accepted that there is equilibrium between the free and albumin-bound bilirubin. When the free bilirubin is removed by adsorbent, more bilirubin will be released from albumin to reach a new equilibrium, until the total adsorption equilibrium is reached between the free bilirubin, the albumin-bound bilirubin and the adsorbent.[42]
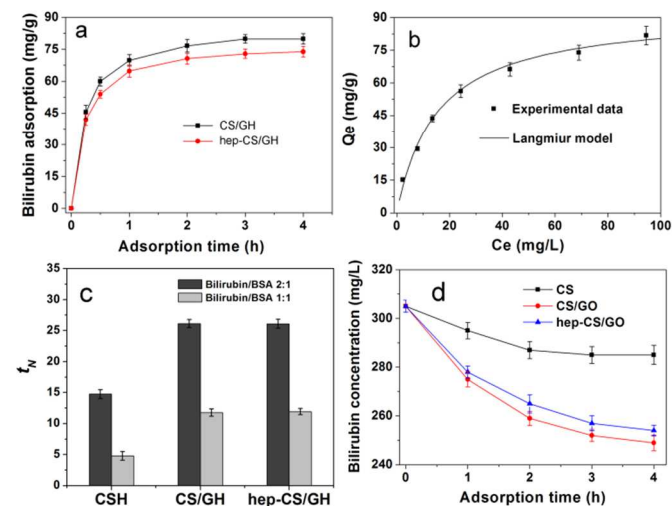
Fig. 5 (a) Adsorption capability of bilirubin by CS/GH and hep-CS/GH as a function of contact time, (b) Adsorption isotherm of bilirubin on hep-CS/GH, (c) t_N values of the hydrogels in bilirubin-enriched abumin solutions, (d) Adsorption of bilirubin from bilirubin-enriched serum at the initial bilirubin concentration of 305.5 mg/L (mean ± S.D, n = 3).

To evaluate the bilirubin adsorption ability of hep-CS/GH in a more complex solution, bilirubin-enriched serum was used to mimic the plasma of hyperbilirubinemia, because serum almost has the same components with plasma but in lack of fibrinogen. Both Fig. 5d and Fig. S7 show that bilirubin concentration decreased progressively with extending adsorption time when the initial bilirubin concentrations were 305.5 mg/L and 153.4 mg/L, respectively, indicating that hep-CS/GH could remove bilirubin from serum at a wide range of bilirubin concentration. For concentration of 305.5 mg/L, after 4 h of adsorption, about 18.4% and 16.7% of bilirubin were removed by CS/GH and hep-CS/GH, respectively, while only 6.5% by pure chitosan hydrogel CSH. This result suggested that incorporation of GO

could enhance the adsorption ability of the hydrogel for bilirubin in serum as well. The adsorption capacity of hep-CS/GH slightly decreased by 9.2% compared with that of CS/GH, and the possible reason has been discussed above. Moreover, the adsorption capacity of hep-CS/GH for bilirubin in serum (8.96 mg/g) was much lower than that in PBS solution (80.3 mg/g), partly because albumin in serum can bind bilirubin. Besides, the adsorbent might also adsorb proteins or other substances in the bilirubin-enriched serum, which may weaken the binding capability of the hep-CS/GH. However, albumin and total protein concentrations only slightly decreased (< 4%) for hep-CS/GH (Table S2), while 16.7% of bilirubin was adsorbed by hep-CS/GH, indicating that bilirubin was preferentially adsorbed on hep-CS/GH in its free form other than bilirubin-albumin conjugates.

Hemocompatibility of the hybrid hydrogel

The adsorption of proteins is the initial event to occur when a biomaterial contacts the blood, which has an influence on further biological processes, such as cell adhesion or activation of enzyme cascades of coagulation.[43] The lower adsorption of proteins often represents the better hemocompatibility.[44] To accurately illustrate the effect of heparin coupling on protein adsorption, protein solutions with low concentration (1 mg/mL) were firstly used. Albumin, the most abundant protein in plasma, and fibrinogen, the most important protein related to blood coagulation, were used as model proteins (Fig. 6a). The protein adsorption capacities of CS/GH for albumin and fibrinogen were higher than those of CSH, which might be due to the adsorption of protein on GO. Previous research has shown that GO could adsorb plasma proteins.[45] After heparin was coupled, the protein adsorption capacities were significantly declined, attributing to the electrostatic repulsion between the negatively charged heparin and the negatively charged albumin or fibrinogen.[46]
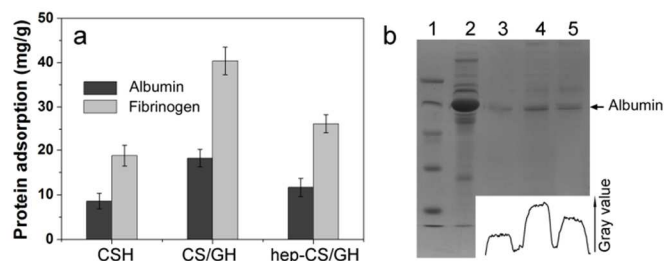
Fig. 6 Protein adsorption by CSH, CS/GH, and hep-CS/GH: (a) albumin and fibrinogen adsorption with the initial concentration of 1 mg/mL (mean ± S.D, n = 3), (b) plasma protein adsorption analyzed by SDS-PAGE image (line 1, protein markers; line 2, plasma; line 3-5, eluted plasma proteins from CSH, CS/GH, and hep-CS/GH, respectively; inset is the gray value of the albumin bands).

Thereafter, plasma protein adsorption was further carried out. The adsorbed plasma protein was eluted with SDS solution and analyzed by SDS-PAGE. Fig. 6b shows that albumin was significantly adsorbed on CSH, CS/GH and hep-CS/GH, because albumin is the most abundant protein in plasma. Other important proteins, such as IgG and fibrinogen, cannot be seen in the SDS-PAGE image, possibly because their adsorption was very low and the gray value of their bands was too low to be detected. The gray value of the albumin band eluted from hep-CS/GH was lower than that of CS/GH (inset of Fig. 6b), indicating a lower albumin adsorption, which was consistent

with the above results. These results show that hep-CS/GH had a better ability of resisting protein adsorption than CS/GH, indicating a better hemocompatibility.

Platelets adhesion on the surface of biomaterials is a crucial event in blood coagulation. The amount of platelets adhered on CSH, CS/GH, and hep-CS/GH was $2.10 \pm 0.39 \times 10^5$, $2.21 \pm 0.72 \times 10^5$, and $0.36 \pm 0.14 \times 10^5$ cells/mm^2 (mean ± SD, n = 6), respectively, quantified by counting the platelets adhered on each sample from six randomly selected SEM images. Significant reduction of platelet adhesion was observed on hep-CS/GH compared with CSH and CS/GH ($p < 0.05$). Fig. 7a-c show the typical SEM images of platelets adhered on the hydrogels. Obviously, numerous platelets were adhered on the surfaces of CSH (Fig. 7a) and CS/GH (Fig. 7b), and a lot of pseudopodium was observed, showing the adherent platelets were in a high degree of aggregation and activation. However, as for hep-CS/GH (Fig. 7c), platelets adhesion and activation were significantly reduced. Heparin is commonly used as an anticoagulant agent, and there are many studies showing a significant reduction of platelet adhesion on heparin-immobilized substrate.[27, 46] A proposed mechanism is probably owing to the electrostatic repulsion between the negatively charged heparin and the cell membrane of platelets.[41] Besides, compared with CS/GH, the ability of resisting protein adsorption of hep-CS/GH may also contribute to the reduction of platelets adhesion, since the adsorption of some plasma proteins could mediate and trigger platelet adhesion and activation, leading to thrombogenesis.[44] It should be noticed that CSH had a lower protein adsorption but a higher platelets adhesion than hep-CS/GH. Since the content of GO (9.09 wt.%) was much less than that of chitosan, it is reasonable to believe that GO was mainly surrounded by chitosan. Once hep-CS/GH came into contact with PRP, proteins (with several to tens of nanometers) could diffuse into the chitosan and be adsorbed on the surface of GO. As a result, GO in hep-CS/GH can cause a higher protein adsorption, while platelets with a larger size of about 2 μm could only mainly contact chitosan. Moreover, heparin coupling to chitosan could reduce protein adsorption on chitosan, so hep-CS/GH had a lower platelets adhesion than CSH.
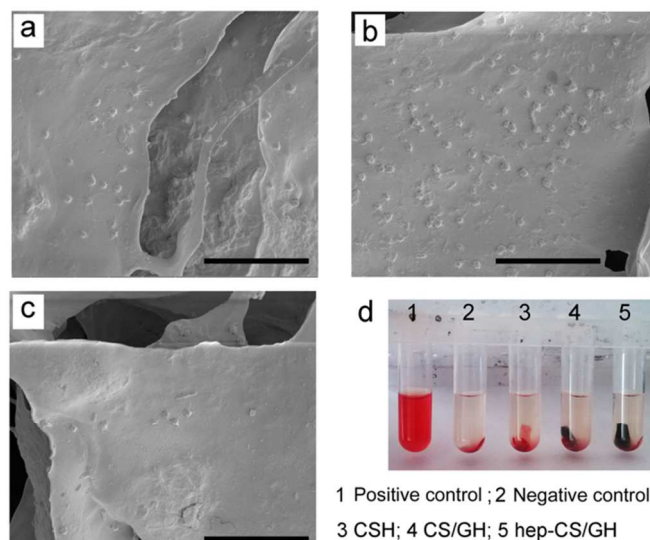
Fig. 7 SEM images of platelet adhesion (scale bar 20 μm): (a) CSH, (b) CS/GH, and (c) hep-CS/GH. (d) Digital image of hemolysis test.

1 Positive control ; 2 Negative control ;
3 CSH; 4 CS/GH; 5 hep-CS/GH

The plasma clotting time was measured to evaluate the anticoagulant ability of the hydrogel (Table 1). The PRT results were basically consistent with the results of platelets adhesion. For CSH and CS/GH, their PRTs were slightly decreased compared with the blank control (6.7 min). After heparin coupling, the PRT of hep-CS/GH was elongated to 23.6 min, which exhibited improved plasma anticoagulant activity, since heparin can specifically interact with antithrombin III to impair the activity of thrombin. For this reason, the formation of fibrin from fibrinogen was suppressed in the presence of heparin. This result means that the dose of heparin administrated by intravenous injection could be lowered in the practical application, which would reduce the risk of bleeding or other severe side effects. Hemolysis is another issue related to the hemocompatibility of biomaterials in contact with blood. Table 1 and Fig. 7d show the degree of hemolysis obtained with CSH, CS/GH, and hep-CS/GH. All the samples demonstrated low degree of hemolysis (< 2%); but still, the heparin-modified hydrogel further reduced the degree of hemolysis.

Table 1. PRTs and the degree of hemolysis of the hydrogels (mean ± S.D, n = 3).

Samples	PRTs (min)	Hemolysis (%)
control	6.7 ± 0.8	——
CSH	5.5 ± 0.6	1.73 ± 0.35
CS/GH	4.1 ± 0.9	1.98 ± 0.47
hep-CS/GH	23.6 ± 1.2	0.92 ± 0.32

There is a trade-off between adsorption performance and anticoagulant activity when designing anticoagulant adsorbents. To realize anticoagulant activity, bioactive or bioinert molecules (such as heparin and PEG) need to be immobilized on adsorbents, which may decrease the adsorption performance towards toxins. Previous researches only focused on improving the adsorption performance of adsorbents. In our work, we focused on improving the anticoagulant activity of the adsorbent and at the same time making its adsorption performance outperforms many other adsorbents. On the whole, hep-CS/GH showed improved hemocompatibility, especially the anticoagulant activity, making it more suitable for contact with blood as a hemoperfusion absorbent. Moreover, due to the excellent mechanical flexibility, the morphology of hep-CS/GH can be regulated or cut into various forms, such as cylinder or film, which can match well with and be directly put in hemoperfusion columns. Besides, hep-CS/GH may also have the adsorption ability for other hydrophobic blood toxins related with liver disease, such as bile acid and tryptophan.[5] Therefore, the development of hep-CS/GH is a significant step towards improving the performance of the adsorbent for blood toxins removal.

Conclusions

In this study, a lyophilization-neutralization-modification method has been proposed to prepare a heparin-modified chitosan/GO hybrid hydrogel for bilirubin adsorption in hemoperfusion. The lyophilization-neutralization process made the chitosan matrix of the hydrogel displayed a foam-like porous structure and excellent mechanical flexibility, which allowed for large deformation and shape recovery.

Incorporating GO into the hydrogel not only improved the compressive strength and Young's modulus, but also significantly increased the adsorption capacity for bilirubin. The maximum adsorption capacity of hep-CS/GH for bilirubin was 92.6 mg/g according to Langmuir isotherm model. We demonstrated that hep-CS/GH performed high adsorption selectivity for bilirubin against albumin, and could effectively adsorb bilirubin from bilirubin-enriched serum. Furthermore, heparin coupling to the hydrogel could improve the hemocompatibility by decreasing plasma protein adsorption, inhibiting platelet adhesion, prolonging PRT, and reducing the degree of hemolysis. Therefore, this study may pave a significant way for improving the performance of the adsorbent for blood toxins removal in hemoperfusion.

Acknowledgements

Notes and references

[a] School of Life Science and Biotechnology, Dalian University of Technology, Dalian 116023, P. R. China. E-mail: lyj81@dlut.edu.cn
[b] Carbon Research Laboratory, State Key Lab of Fine Chemicals, School of Chemical Engineering, Dalian University of Technology, Dalian 116023, P. R. China.

Electronic Supplementary Information (ESI) available: Descriptions of adsorption isotherm models, parameters of Langmuir and Freundlich isotherms, protein concentrations in serum before and after adsorption, chemical structure of bilirubin, schematic illustration of the equipment for the compressive test, optical microscopy images of the hydrogels, XRD patterns, elemental mapping image of S for CS/GH, digital images of shape recovery of the hep-CS/GH, and adsorption of bilirubin from bilirubin-enriched serum at the initial bilirubin concentration of 153.4 mg/L. See DOI: 10.1039/b000000x/

1   Y. Takenaka, *Ther. Apher.,* 1998, **2**, 129-133.
2   G. J. Tao, L. X. Zhang, Z. L. Hua, Y. Chen, L. M. Guo, J. M. Zhang, Z. Shu, J. H. Gao, H. R. Chen, W. Wu, Z. W. Liu and J. L. Shi, *Carbon*, 2014, **66**, 547-559.
3   B. R. Muller, *Carbon,* 2010, **48**, 3607-3615.
4   L. M. Guo, J. M. Zhang, Q. J. He, L. X. Zhang, J. J. Zhao, Z. Y. Zhu, W. Wu, J. Zhang and J. L. Shi, *Chem. Commun.*, 2010, **46**, 7127-7129.
5   V. Weber, I. Linsberger, M. Hauner, A. Leistner, A.Leistner and D. Falkenhagen, *Biomacromolecules*, 2008, **9**, 1322-1328.
6   K. Shinke, K. Ando, T. Koyama, T. Takai, S. Nakaji and T. Ogino, *Colloids Surf. B*, 2010, **77**, 18-21.
7   T. Tang, Y. L.Zhao, Y. Xu, W. Dong, J. Xu and F. Deng, *Appl. Surf. Sci.*, 2011, **257**, 6004-6009.
8   R. D. Frank, U. Muller, R. Lanzmich, C. Groeger and J. Floege, *Nephrol. Dial. Transplant*, 2006, **21**, 1013-1018.
9   H. Ren, D. D. Kulkarni, R. odiyath, W. Xu, I. hoi and V. V. Tsukruk, *ACS Appl. Mater. Interfaces*, 2014, **6**, 2459-2470.
10 Y. Gao, Y. Li, L. Zhang, H. Huang, J. Hu, S. M. Shah and X. Su, *J. Colloid Interf. Sci.*, 2012, **368**, 540-546.
11 N. A. Travlou, G. Z. Kyzas, N. K. Lazaridis and E. A. Deliyanni, *Langmuir*, 2013, **29**, 1657-1668.
12 J. N. Tiwari, K. Mahesh, N. H. Le, K. C. Kemp, R. Timilsina, R. N.Tiwari and K. S. Kim, *Carbon*, 2013, **56**, 173-182.
13 C. Cheng, S. Li, S. Nie, W. Zhao, H. Yang, S. Sun, and C. Zhao, *Biomacromolecules*, 2012, **13**, 4236-4246.

14 K. H. Liao, Y. S. Lin, C. W. Macosko and C. L. Haynes, *ACS Appl. Mater. Interfaces*, 2011, **3**, 2607-2615.

15 A. Sasidharan, L. S. Panchakarla, A. R. Sadanandan, A. Ashokan, P. Chandran, C. M. Girish, D.Menon, S. V. Nair, C. N. R. Rao and M. Koyakutty, *Small*, 2012, **8**, 1251-1263.

16 W. Chen and L. Yan, *Nanoscale*, 2011, **3**, 3132-3137.

17 C. Huang, H. Bai, C. Li and G. Shi, *Chem. Commun.*, 2011, **47**, 4962-4964.

18 H. Bai, C. Li, X. Wang and G. Shi, *J Phys. Chem. C*, 2011, **115**, 5545-5551.

19 H. Bai, K. Sheng, P. Zhang, C. Li and G. Shi, *J Mater. Chem.*, 2011, **21**, 18653-18658.

20 Y. Xu, Q. Wu, Y. Sun, H. Bai and G. Shi. *ACS Nano*, 2010, **4**, 7358-7362

21 V. Balan and L. Verestiuc, *Eur. Polym. J.*, 2014, **53**, 171-188.

22 N. Zhang, H. Qiu, Y. Si, W. Wang and J. Gao, *Carbon*, 2011, **49**, 827-837.

23 Y. Wang, X. Liu, H. Wang, G. Xia, W. Huang and R. Song, *J. Colloid Interf. Sci.*, 2014, **416**, 243-251.

24 Y. Chen, Y. Qi, X. Yan, H. Ma, J. Chen, B. Liu and Q. Xue, *J. Appl. Polym. Sci.*, 2014, **131**, 40006.

25 Y. Chen, L. Chen, H. Bai and L. Li, *J. Mater. Chem. A*, 2013, **1**, 1992-2001.

26 M. S. Lord, B. Cheng, S. J. McCarthy, M. Jung and J. M. Whitelock, *Biomaterials*, 2011, **32**, 6655-6662.

27 X. Liu, L. Yuan, D. Li, Z. Tang, Y. Wang, G. Chen, H. Chen and J. L. Brash, *J. Mater. Chem. B*, 2014, **2**, 5718-5738.

28 H. Hu, Z. Zhao, Q. Zhou, Y. Gogotsi and J. Qiu, *Carbon*, 2012, **50**, 3267-3273.

29 H. Hu, Z. Zhao, W. Wan, Y. Gogotsi and J. Qiu, *ACS Appl. Mater. Interfaces*, 2014, **6**, 3242-3249.

30 H. Wei, L. Han, J. Ren and L. Jia, *ACS Appl. Mater. Interfaces*, 2013, **5**, 12571-12578.

31 D. Han and L. Yan, *ACS Sustainable Chem. Eng.*, 2014, **2**, 296-300.

32 L. Qiu, J. Z. Liu, S. L. Y.Chang, Y.Wu and D. Li, *Nat. Commun.*, 2012, **3**, 1241.

33 J. Wang, W. Hu, Q. Liu and S. Zhang, *Colloids Surf. B*, 2011, **85**, 241-247.

34 H. P. Cong, P. Wang and S. H. Yu, *Small*, 2014, **10**, 448-453.

35 Z. Cui, A. H. Milani, P. J. Greensmith, J. Yan, D. J. Adlam, J. A. Hoyland, I. A. Kinloch, A. J. Freemont and B. R. Saunders, *Langmuir*, 2014, **30**, 13384-13393.

36 C. Rodriguez-Gonzalez, A. L. Martinez-Hernandez, V. M. Castano, O. V. Kharissova, R. S. Ruoff and C. Velasco-Santos, *Ind. Eng. Chem. Res.*, 2012, **51**, 3619-3629.

37 Y. H. Yu and B. L. He, *React. Funct. Polym.*, 1996, **31**, 195-200.

38 L. Guo, L. Zhang, J. Zhang, J. Zhou, Q. He, S. Zeng, X. Cui and J. Shi, *Chem. Commun.*, 2009, 6071-6073.

39 L. Wu and Z. Zhang, *J. Appl. Polym. Sci.*, 2013, **130**, 563-571.

40 M. E. Avramescu, W.F.C. Sager, Z. Borneman and M. Wessling, *J. Chromatogr. B*, 2004, **803**, 215-223.

41 M. Xue, Y. Ling, G. Wu, X. Liu, D. Ge and Wei Shi, *J. Chromatogr. B*, 2013, **912**, 1-7.

42 T. Tang, X. Li, Y. Xu, D. Wu, Y. Sun, J. Xu and F. Deng, *Colloids Surf. B*, 2011, **84**, 571-578.

43 C. Werner, M. F. Maitz and C. Sperling, *J. Mater. Chem.*, **2007**, 17, 3376-3384.

44 Y. Chang, W. J. Chang, Y. J. Shih, T. C. Wei and G. H. Hsiue, *ACS Appl. Mater. Interfaces*, 2011, **3**, 1228-1237.

45 H. M. Kim, K. M. Kim, K. Lee, Y. S. Kim and J. M. Oh, Eur. *J. Inorg. Chem.*, 2012, 5343-5349.

46 C. J. Pan, Y. H. Hou, B. B. Zhang, Y. X. Dong and H. Y. Ding, *J. Mater. Chem. B*, 2014, **2**, 892–902.

Graphic abstract
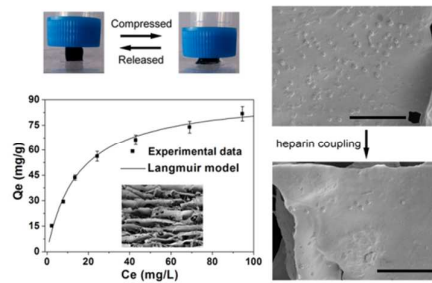
A highly flexible heparin-modified chitosan/graphene oxide hydrogel was prepared *via* lyophilization-neutralization-modification as a blood compatible adsorbent for bilirubin removal.